10th International Conference on Fracture Mechanics of Concrete and Concrete Structures
FraMCoS-X
G. Pijaudier-Cabot, P. Grassl and C. La Borderie (Eds)
https://doi.org/10.21012/FC10.235704

LATTICE MODEL FOR NUMERICAL ANALYSIS OF FRACTURE PROCESS OF CONCRETE MATERIAL UNDER VARIOUS LOADING CONDITIONS

ZE CHANG, HONGZHI ZHANG, ERIK SCHLANGEN AND BRANKO ŠAVIJA

*Delft University of Technology
Delft, Netherlands
e-mail: {z.chang-1; h.zhang-5; erik.schlangen; b.savija}@tudelft.nl

Key words: Fracture process, 3D Lattice model, Boundary condition

Abstract: The aim of this work is to investigate the fracture process of concrete under various boundary conditions. Although numerous concrete fracture tests have been reported, showing the failure behavior of concrete, their evaluation is ambiguous due to the limitations of specimen size and experimental conditions. Therefore, it is necessary to use simulation models to better understand the fracture process. This is done herein by using a three-dimensional lattice model to simulate the failure behavior of concrete under different loading conditions ranging from uniaxial compression, tension, splitting, three point bending to shear by using a single set of input parameter. In addition, several influence factors including boundary condition and slenderness are also taken into consideration to give more detailed information about the fracture process of concrete.

1 INTRODUCTION

Concrete, a typical porous and anisotropic material, has complicated fracture mechanisms due to its microstructure [1,2]. It is generally accepted that cracking within concrete usually forms and propagates in a direction which is perpendicular to the maximum tensile stress [3,4]. During the process of crack propagation, the stress distribution caused by loading (external loading or internal loading) determines the final crack pattern together with the mechanical properties of the specimen. Therefore, understanding the deformation and fracture performance of concrete under various loading conditions is of importance for research and engineering practice.

Numerical tools are an excellent choice to gain deeper insight of into these problems. Numerical modelling of concrete failure has experienced a great progress in the past decades. There are several modelling approaches for concrete fracture including but not limited to finite element method (FEM), extended finite element method (XFEM) [5,6], discrete element model [7], smeared crack model, and lattice discrete element model [8,9]. Based on the continuum theories, FEM is usually utilized to simulate the crack propagation. In order to better understand the fracture behaviour of anisotropic materials and simulate the cracks via discontinuity-based method, several discrete element models were proposed. Among these models, the medium can be discretized by introducing the particles or lattice beams.

The lattice model was first proposed by the Hrennikoff [10]. Lattice discrete element model, in which one-dimensional element is utilized to represent structural continuum, emerged as an attractive alternative to continuum approaches to model cementitious materials and structures. In the 1980s, the lattice model was perfected by adding related theoretical physics to study the fracture behaviour of the material with high disorder [11]. Then, Zubelewicz and Bažant [12]

presented to use bidimensional particles assembly to study the fracture process of quasi-brittle materials. Almost in the same time, Schlangen and Van Mier [13] proposed lattice fracture model to compensate the drawbacks of discrete and smeared crack FE model . More recently, such lattice model was utilized to study the fracture behaviour of cementitious materials such as concrete. It is generally accepted that the classical lattice uses the truss or beam elements to interconnect on the positioned points through triangle or quadrilateral method. When the positioned points are irregular, this construction method can implement the heterogeneity of the materials [2]. It is also possible to achieve it by assigning randomness local mechanical properties to different lattice beam elements [3]. Alternatively, the anisotropy of material can be achieved by mapping an image about material structure produced by computed tomography scanning, dynamical processes or random generators, to the available lattice model. Using this method, a simulation model very similar to the real material can be obtained.

In this paper, the use of a three-dimensional lattice model for simulating fracture process of concrete under different boundary conditions ranging from uniaxial compression, tension, splitting, three point bending to shear by using a single set of input parameter was presented. The tendency of load displacement curve and failure mode were compared with experimental results. Based on it, several factors (i.e. boundary condition, load area, size effect) were also taken into consideration to show the influence to the final failure mode.

2 DESCRIPTION OF LATTICE MODEL

In this paper, the lattice model is constituted by brittle-breaking beam elements through triangle method. The triangular lattice is the essential for this model since it can give the least chance for preferential crack directions [3]. Node and mesh generation procedure of 3D lattice model is shown in Figure 1.

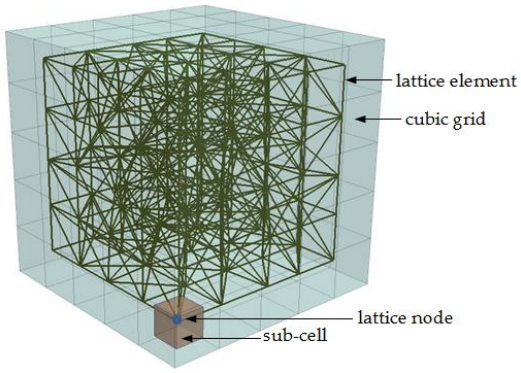

Figure 1: Node and mesh generation procedure of 3D lattice model

3 FRACTURE PROCESS

In lattice fracture analysis, both displacement and loading could be regarded as boundary condition and imposed on the system. For every step, the element with the highest stress/strength ratio is removed and the inverse of this ratio is defined as the system scaling factor [2]. Once the critical element is found, the whole stiffness matrix is updated due to the damage. The step-by-step removal of critical lattice element present the initiation and propagation of the crack, finally, crack pattern of the lattice model could be obtained. Meanwhile, the displacement of the model, calculated by scaling factor and prescribed displacement, determines the load displacement curve of the model together with the reaction force.

On the basis of the Timoshenko beam theory, the element is a lattice beam of uniform cross-section and can transfer the uniaxial force, shear, bending and torsion [14]. The stress for the lattice element is calculated by the following equation.

$$\sigma = \frac{F}{A} + \alpha \frac{\left(|M_i|, |M_j|\right)_{\max}}{W} \qquad (1)$$

Where F is the normal force for the lattice beam element, A is the cross-sectional area of an element, and $W=\pi D^3/32$ (D is the diameter of the circle area). The coefficient α is the bending influence factor which balances the final failure mode in which either force or bending plays a dominate role.

In the previous 2D analyses, the contribution of the bending moment to the

critical stress in the beam is taken into consideration by the value α=0.005 [15-17]. In [15], it is shown that the change of the α parameter affects the tail in the stress-deformation curve. The large α shows a more brittle global behavior whereas, the small α gives a long tail in the load and displacement response, in particular, the fracture process shows a peeling effect when α is equal to 0 [18]. In order to better understand the influence of α on the 3D lattice analysis, several analyses about uniaxial tension and compression with different values of α (0, 0.25, 0.5,0.75,1) has been conducted to search for the effect of α on load-displacement curve and final failure mode. The results from these analyses are summarized in the following.

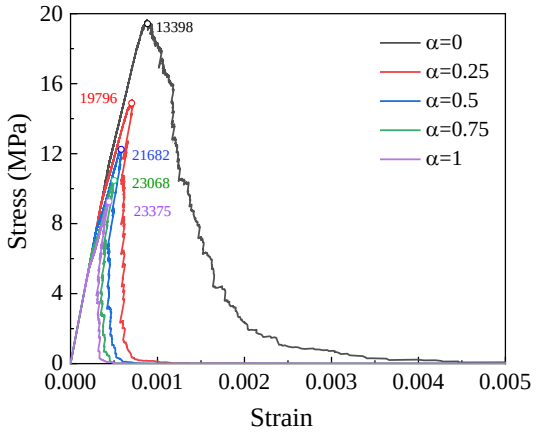

Figure 2: Load-displacement curve for different bending influence factors

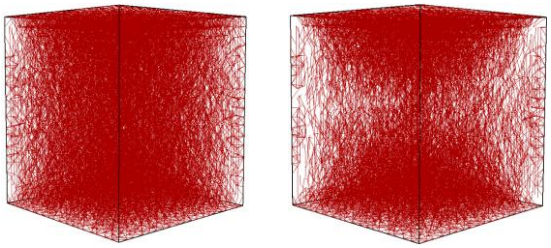

(a) step=19796 (b) final failure mode

Figure 3: Fracture process of the model with α=0.25

It can be seen from Figure 2 and Figure 3 that both the load displacement curve and failure mode of the model (α=0.25) show the similar tendency with experimental results. Thus, in the following section, α was taken as 0.25 to conduct the analyses.

After solving liner algebraic equations to get the node displacement, the stress for lattice beam element is obtained. Then the system scaling factor is calculated and the critical element was determined. The system scaling factor, together with the reactions on the restraint boundaries, determines the load displacement curve.

4 NUMERICAL ANALYSIS

In this part, all simulations ranging from uniaxial tension and compression, splitting test, three point bending test to double edge notched (DEN) beam shear test were conducted using a single input parameter including the bending influence factor, the local mechanical property (i.e. elastic modulus, shear modulus, tensile strength and compressive strength). One point should be noted that all input parameters keep the same except for the model size.

In this paper, in order to remove the influence from other factors (coarse aggregate distribution and grading) and taking into account the computer resources, the model was considered as homogeneous, and the compressive strength and tensile strength were taken as 30MPa and 3MPa, respectively. The elastic modulus and shear modulus were set to 25GP and 10GP, respectively. Other input parameter values used in this paper are summarized in Table 1.

Table 1 Details about the input parameters for numerical analysis

Simulation test	Model size (mm×mm×mm)	α	Resolution
Uniaxial compression	20×20×20	0.25	1mm
Uniaxial tension	20×20×20	0.25	1mm
Splitting	25×25×25	0.25	1mm
Three-point bending	113×20×10	0.25	1mm
DEN shear	128×12×48	0.25	1mm

4.1 Uniaxial compression and tension test

The model was loaded under constant strain rate conditions. In fact, the loading was applied by the displacement set on the upper boundary. The other direction displacements

were fixed to simulate the high friction between the specimen and the machine in the experiment. The simulation models are shown in Figure 4, and the failure evaluations of compression simulation and tension simulation are shown in Figure 5. The load displacement response of the lattice model under uniaxial compression and tension is plotted in Figure 6.

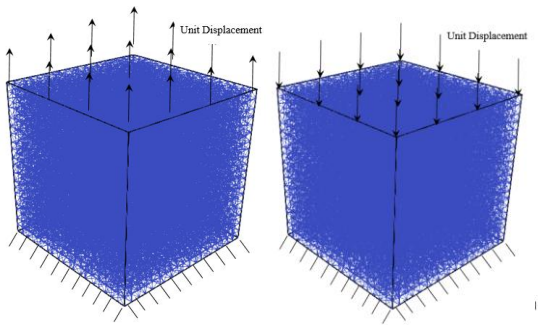

(a) tension (b) compression

Figure 4 Examples of boundary conditions used for uniaxial compression and tension modelling.

The fracture process of both uniaxial compression and tension simulation agrees qualitatively well with the observations in experiment with high friction condition. In compression, following a localization of deformations on diagonal bands within the specimen, the failure elements started to orient on the main diagonals connecting the edges of the specimen. The loss of lateral stiffness due to progressive beam breaking in the horizontal direction lead to bulging of the model. Finally, the broken element connected each other to form a diagonal main crack shown in Figure 5 (a). For tension simulation, micro-cracks occurred in the beginning. Then, a main crack forms close to the middle of the specimen, as shown in Figure 5 (b). Meanwhile, the load displacement curve changed during the propagation of the main crack. Once the main crack passed through the whole specimen, the capacity of bearing the tension load lost. Finally, the final failure mode happened with an obvious main crack.

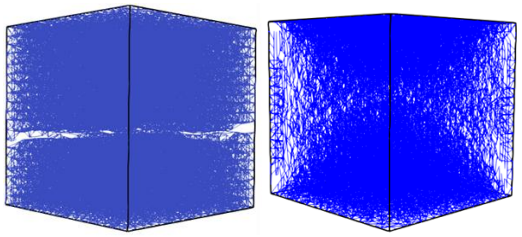

(a) tension (b) compression

Figure 5: The final failure mode of concrete exposed to uniaxial loading (the white is crack and the blue is solid material)

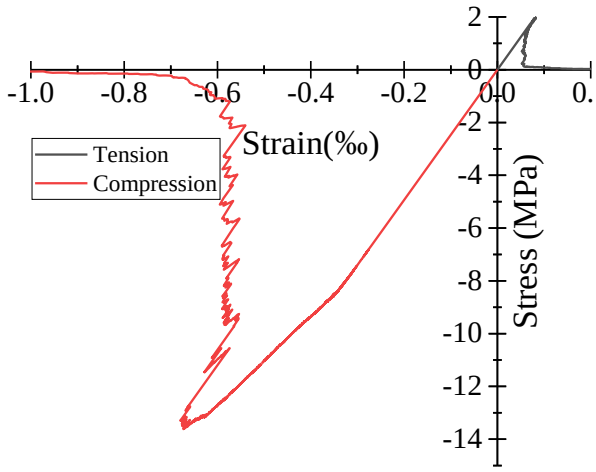

Figure 6 The stress and strain curve of concrete exposed to uniaxial loading

4.2 Effect of model slenderness and boundary condition

Evidence of existing experiments [19] showed that the boundary conditions and slenderness affects the fracture process and load displacement curve in uniaxial compression. In order to see if the model is able to reproduce the effect of the boundary condition and slenderness, the following simulations were performed.

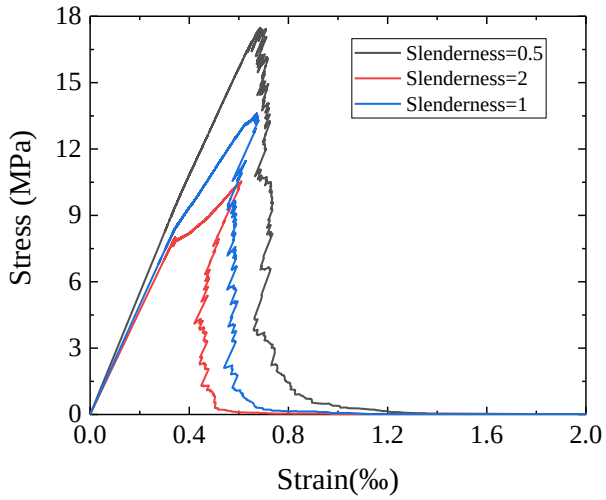

(a) Stress strain curve for high friction

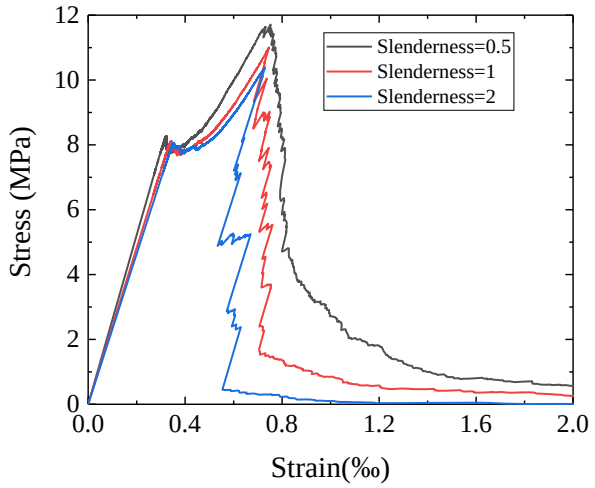

(b) Stress strain curve for low friction

Figure 7 Stress strain curves for compression test under different boundary conditions

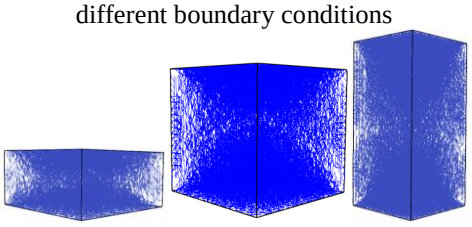

(a) High friction boundary condition (white denotes the crack)

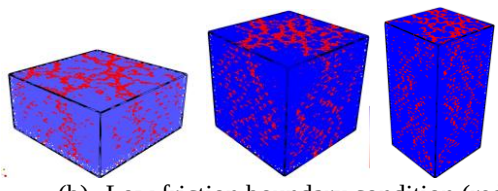

(b) Low friction boundary condition (red denotes the crack)

Figure 8 Failure behavior of concrete in compression with different boundary conditions

In Figure 7, the stress-strain curves are plotted for models with various slenderness and different boundary conditions. For high friction boundary condition, the slenderness had a significant influence on the peak load, values for both peak load and strain at the peak stress increased with the decreasing model height. For low friction boundary condition, the change of slenderness had a very small influence on the peak load and strain at the peak load. Meanwhile, the peak load for high friction boundary condition was higher than for the free boundary since the high friction could constrain the lateral deformation and improve the bearing capacity. Figure 8 shows the final failure modes for the high friction and the low friction boundary condition. For the models with slenderness equal to 1, the failure mode of the model with low friction were characterized by localized cracks almost parallel to the applied load, besides, a huge number of elements from upper and lower surfaces broke. However, for the same model with high friction boundary condition, failure mode was characterized by inclined cracks that leaved the model end almost undamaged and had less opening than the free boundary condition. Furthermore, compared with high boundary condition, many micro-cracks happened on the upper and bottom area during the fracture process due to the free friction. This is in accordance with experimental observations [20].

4.3 Three-point bending test

In this section, numerical analyses of the three-point bending test were carried out to evaluate the ability of lattice to simulate the fracture behavior in flexure. In order to take into consideration of the size effect, three models, height, equal 10mm, 20mm, 30mm, respectively, length, 139mm, 113mm, 80mm, respectively, were created, and one of models is shown in Figure 9. The thickness of the beams was 10 mm for all the three sizes. All of these models are notched with half-depth 2mm width notches. With regard to the

loading, displacement was applied to the middle line of the upper area and two lines of nodes at the bottom were fixed, one side with 3 translational directions, and the other one only in vertical direction.

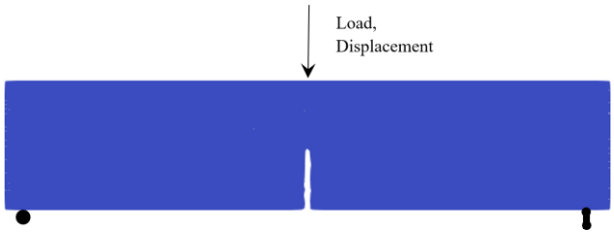

Figure 9 Geometry of three-point bending test specimen

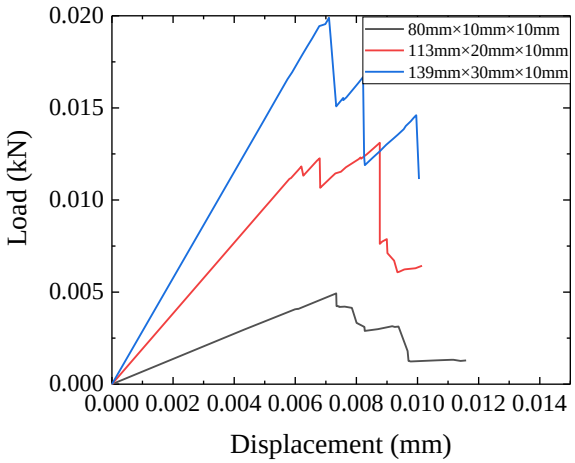

Figure 10 Load displacement curve for three point bending test

Figure 11 Failure mode for three point bending test

It could be seen from Figure 10 that the peak load increased with the increase of the model size and the post peak behavior becomes more ductile. For the fracture process, the crack initial started from the notch and propagated to the upper area along with the almost straight path, as shown in Figure 11. It is also worth noting that the fracture process for different size did not change. This is in agreement with the experiments performed by the Nallathambi et al and the typical evidence reported in the literature [21].

4.4 Splitting test

The splitting test conducted by Bažant et al [22] was modelled in this part. Various sizes of specimens including 15mm, 25mm, 35mm, were created to simulate the size effect. The simulation is shown in Figure 12**.** Figure 13 shows the nominal stress, calculated as $2P/(\pi L^2)$, versus displacement curve obtained in the numerical simulation.

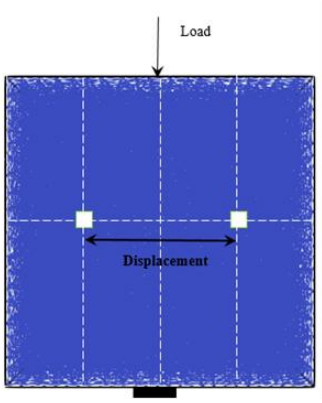

Figure 12 Geometry of splitting test specimen

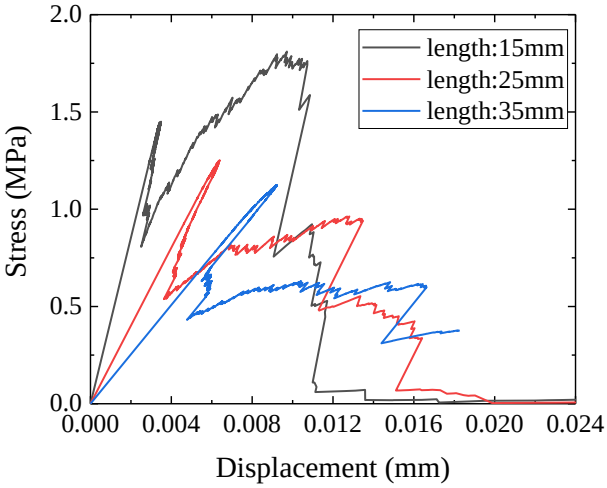

Figure 13 Stress and displacement curve for splitting test

Figure 14 Fracture behaviour for splitting test

Figure 14 shows the crack pattern from the splitting simulation. The results show that the peak nominal stress decreases with the increasing size. With respect to the failure mode, the size had a small influence on fracture process. In general, the crack initiated in the middle of the model because of the tension and propagated to the upper and bottom and a main crack formed. However, the peak load obtained by the splitting is lower than the value calculated by uniaxial tension for the same model, which needs to be further studied.

4.5 Double-edged-notch beam shear

The double edge notched (DEN) shear specimen was firstly proposed by the Bažant and Pfeiffer [23] to study the shear fracture of concrete, then, Schlangen [15] conducted the single edge notched (SEN) and DEN beam shear test using a specific test machine. Based on his experiment, the crack generation and propagation are different from high and low friction boundary conditions.

In this section, the numerical analysis about boundary conditions was carried out. The specimen is 128 mm in length, 13 mm in width, 48 mm in height and is shown in Figure 15. Two pre-existing notches with a width of 5 mm and a length of 25 mm are created at the two edges of the model. In the DEN beams, the value of crack mouth opening displacement (CMOD) and the crack mouth sliding displacement (CMSD) at the top and bottom notch on the front of the specimen is used as feed-back signal.

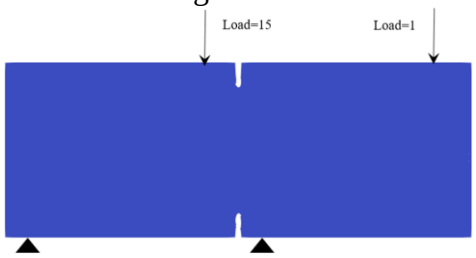

Figure 15 Geometry of DEN beam shear test

For high friction boundary condition, the model with a fixed support loading system instead of freely rotating supports was used and additions constraints were imposed on the rotations of support. In that way, the fixation of the supports introduced a constrains with respect to the horizontal displacement and rotations of the supports. For free boundary condition, the model with freely rotating support was used. Figure 17 illustrates the fracture process of SEN beam under fixed boundary condition. It can be seen that the crack generated from the notch and propagated in a curved shape. Because of the restrain of the horizontal displacement of loading nodes, the double curved crack was arrested due to the new configuration of the horizontal force in the model. Then, a splitting crack arose at the center of the beam and developed to the upper and bottom surface. This is the final failure mode for the high friction boundary condition. Unlike the high friction boundary condition, in the free boundary condition case one of the curved cracks continued propagating due to the lack of the horizontal constraint and reached to the bottom boundary. This was the final failure mode as shown in Figure 17.

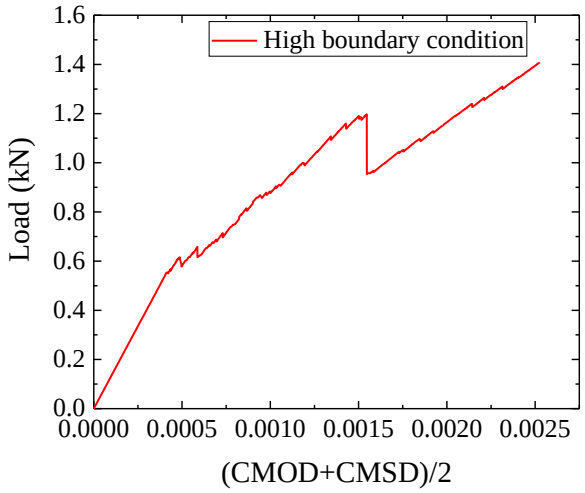

(a) high friction boundary condition

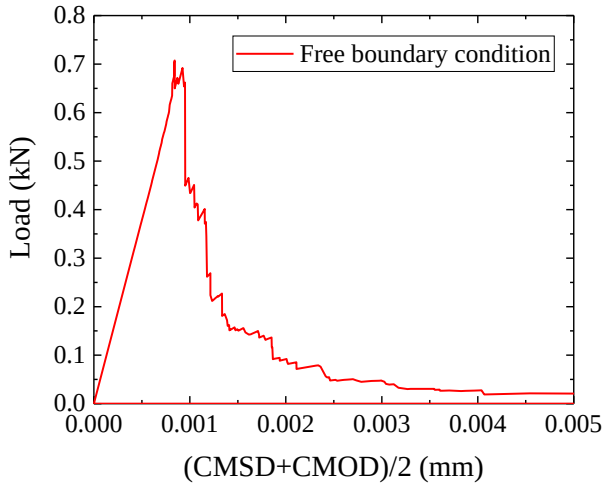

(b) low friction boundary condition

Figure 16 Load displacement curve for DEN exposed to shear with different boundary conditions

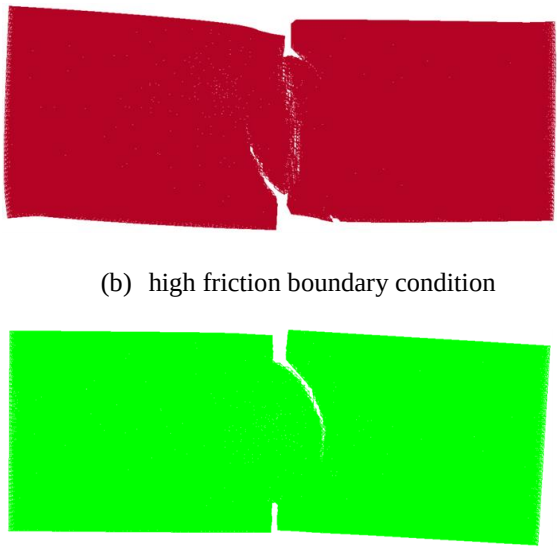

(b) high friction boundary condition

(b) low friction boundary condition

Figure 2 Failure mode for DEN exposed to shear with different boundary conditions

Besides of the fracture process, the load-displacement could be seen from the Figure 16, simulation results about free boundary keep the same tendency with the experimental results obtained by Schlangen [15]. However, the post peak response is too stiff for the high friction boundary condition, most probably because the supports in the experiments were not completely fixed.

5. CONCLUSION

In this paper, a 3D lattice model was utilized to simulate different kinds of experiments ranging from uniaxial compression, tension, splitting, three point bending test to DEN beam shear test using a single set of input parameter.

Based on the results obtained in this study, the following conclusion can be formulated,

- Lattice model can simulate the fracture process of concrete under uniaxial compression and tension. The model captures well the effect of high friction boundary and low friction boundary conditions on compressive strength and post-peak ductility. In addition, lattice model also predicted the difference between the different boundary conditions and slenderness.
- Lattice model accurately simulated concrete subjected to three-point bending test. Besides, it also can predict the fracture process accurately and analyze the size effect on the load displacement curve.
- Lattice model can simulate the fracture process in the Brazilian splitting test and analyze the size influence on the peak load.
- Lattice model has the capacity to simulate the fracture process during a DEN experiment. It not only can predict the crack generation and propagation accurately but also show the influence by different boundary conditions.

One of the most important point for this research, is that various experiments can be simulated by using a single set of parameters. Both the failure mode and load displacement or stress-strain curve show the same results or the same tendency with experiments.

ACKNOWLEDGEMENTS

Ze Chang, and Hongzhi Zhang would like to acknowledge the funding supported by China Scholarship Council under grant number 201806060129 and 201506120067 respectively.

REFERENCES

[1] Cusatis, G., Pelessone, D. and Mencarelli, A., 2011. Lattice Discrete Particle Model

(LDPM) for failure behavior of concrete. I: Theory. *Cem. Concr. Compos.* **33:**881-890.

[2] Qian, Z., Schlangen, E., Ye, G., et al., 2017. Modeling Framework for Fracture in Multiscale Cement-Based Material Structures. *Materials.* **10**:587.

[3] Schlangen, E., and Van Mier, J. G. M., 1992. Simple lattice model for numerical simulation of fracture of concrete materials and structures. *Mater. Struct.* **25:**534-542.

[4] Oliver-Leblond, C., 2019. Discontinuous crack growth and toughening mechanisms in concrete: A numerical study based on the beam-particle approach. *Eng. Fract. Mech.* **207:**1-22.

[5] Sawamoto, Y., Tsubota, H., Kasai, Y., et al., 1998. Analytical studies on local damage to reinforced concrete structures under impact loading by discrete element method. *Nucl. Eng. Des.* **179:**157-177.

[6] Delaplace, A. and Desmorat, R., 2008. Discrete 3D model as complimentary numerical testing for anisotropic damage. *Int. J. Fract.* **148:**115-128.

[7] Zelelew, H. M., and Papagiannakis, A. T. 2010. Micromechanical modeling of asphalt concrete uniaxial creep using the discrete element method. *Road Mater. Pavement Des.* **11:**613-632.

[8] D'Addetta, G. A., Kun, F., and Ramm, E., 2014. On the application of a discrete model to the fracture process of cohesive granular materials. *Granul. Matter.* **4:**77-90.

[9] Sherzer, G., Gao, P., Schlangen, E., et al., 2017. Upscaling Cement Paste Microstructure to Obtain the Fracture, Shear, and Elastic Concrete Mechanical LDPM Parameters. *Materials.* **10**:242

[10] Hrennikoff A., 1941. Solution of problems of elasticity by the framework method. *J. Appl. Mech.* **12**:169-175.

[11] Herrmann H. J., Hansen A., and Roux S., 1989. Fracture of disordered, elastic lattices in two dimensions. *Phys. Rev. B.* **39**:637-648.

[12] Zubelewicz A. and Bažant Z P., 1987. Interface element modeling of fracture in aggregate composites. *J. Eng. Mech.* **113**:1619-1630.

[13] Schlangen, E., and Van Mier, J. G. M., 1992. Experimental and numerical analysis of micromechanisms of fracture of cement-based composites. *Cem. Concr. Compos.* **14**:105-118.

[14] Liu, D., Šavija, B., Smith, G.E., et al., 2017. Towards understanding the influence of porosity on mechanical and fracture behaviour of quasi-brittle materials: experiments and modelling. *Int. J. Fract.* **205:**57-72.

[15] Schlangen, E., 1993. Experimental and numerical analysis of fracture processes in concrete. (Ph.D. thesis). *The Netherlands: Delft University of Technology*.

[16] Van Vliet, M.R.A., 2000. Size effect in tensile fracture of concrete and rock, (Ph.D. thesis). *The Netherlands: Delft University of Technology*.

[17] Lilliu, G., 2007. *3D analysis of fracture processes in concrete*, Eburon Uitgeverij BV.

[18] Tzschichholz, F., 1992. Peeling instability in Cosserat-like media. *Phys. Rev. B.* **45**: 12691-12698.

[19] Carpinteri A, Ciola F, Pugno N, et al., 2001. Size-scale and slenderness influence on the compressive strain-softening behaviour of concrete. *Fatigue Fract. Eng. Mater. Struct.* **24**:441-450.

[20] Van Mier, J. G. M., 2017. *Fracture processes of concrete*, CRC press.

[21] Nallathambi P., Karihaloo B. L. and Heaton B. S., 1985. Various size effects in fracture of concrete. *Cem. Concr. Res.* **15**: 117-126.

[22] Bažant, Z.P., Kazemi, M.T., Hasegawa, T., et al., 1991. Size effect in Brazilian split-cylinder tests: measurements and fracture analysis. *ACI Mater. J.* **88:**325-332.

[23] Bažant, Z. P. and Pfeiffer, P. A. 1986. Shear fracture tests of concrete. *Mater. Struct.* **19:**111-121.